

## Electronic Supplementary Information (ESI)

# Adsorption and Dehydrogenation of Tetrahydroxybenzene on Cu(111)

Fabian Bebensee,<sup>a</sup> Katrine Svane,<sup>a</sup> Christian Bombis,<sup>a</sup> Federico Masini,<sup>a</sup> Svetlana Klyatskaya,<sup>b</sup> Flemming Besenbacher,<sup>a</sup> Mario Ruben,<sup>b,c</sup> Bjørk Hammer,<sup>a</sup> and Trolle Linderoth,<sup>\*a</sup>

<sup>a</sup> Interdisciplinary Nanoscience Center (iNANO) and Department of Physics and Astronomy, Aarhus University, Aarhus C, Denmark. \*E-mail: trolle@inano.au.dk

<sup>b</sup> Department of Physics and Astronomy, Aarhus University, Aarhus C, Denmark.

<sup>c</sup> Karlsruhe Institute of Technology (KIT), Institut für Nanotechnologie, Karlsruhe, Germany.

## 1. Experimental Section

The STM and lab-based XPS experiments were conducted employing a commercially available UHV system (SPECS) with a base pressure in the low  $10^{-10}$  mbar regime. The system incorporates an Aarhus type STM, a non-monochromatic dual anode X-ray source and a hemispherical energy analyzer for XPS. In the experiments discussed in this paper, only the Al-anode was used (excitation energy 1486.6 eV).

THB/DHBQ molecules were sublimated from a quartz crucible placed in a home-build evaporator (Knudsen type) cell at a crucible temperature of 340 K.

THB was obtained according to a literature procedure<sup>[1]</sup> by reduction of 2,5-dihydroxybenzo-quinone (DHBQ) with metallic tin and hydrochloric acid followed by recrystallization from THF. DHBQ (purity >99%) was bought from Sigma Aldrich. All molecules were thoroughly degassed in the crucible prior to use, but not purified further.

All STM images were collected at RT, all XP spectra were collected nominally at RT unless stated otherwise. Here, nominal RT refers to the sample not being actively heated or cooled – by placing the X-ray source close to the surface, the sample temperature typically stabilised at around 320 K during measurements.

## 2. DHBQ on Cu(111)

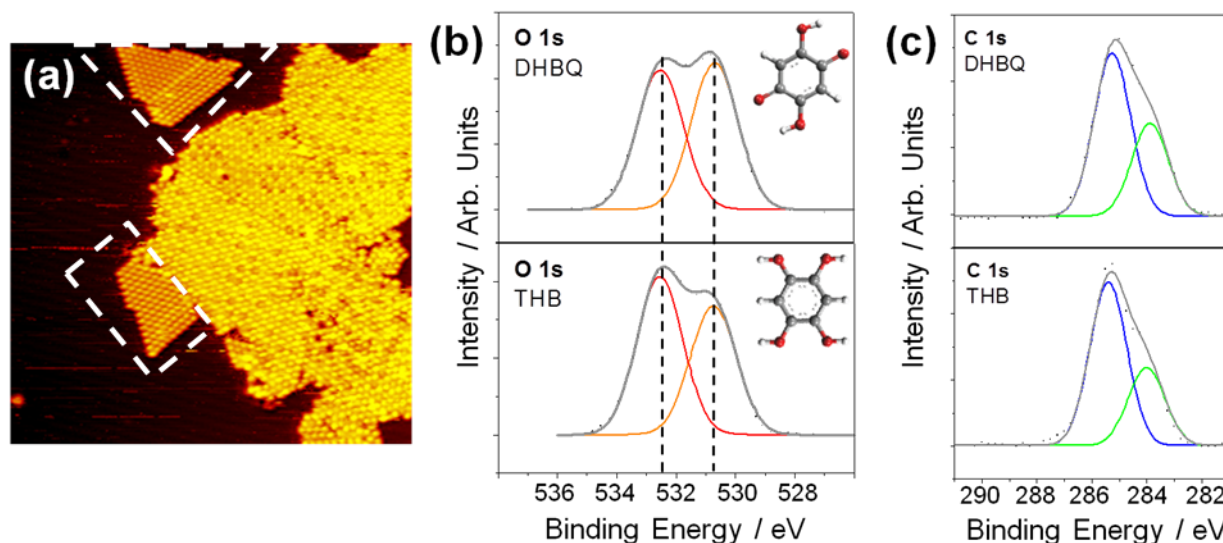


**Fig. S1** STM image ( $I_T$  0.33 nA,  $U_T$  -1.63 V) (a) with the single layer islands highlighted by white dashed lines and XP spectrum of the O 1s region (b) and C 1s region (c) of DHB adsorbed on Cu(111) at RT. For comparison, corresponding spectra of THB annealed to 370 K are also shown in the bottom of (b) and (c).

Fig. S1 displays the result of a control experiment, where DHBQ was deposited on a Cu(111) substrate at room temperature. Apart from the tendency to form double layers on Cu(111), DHBQ adapts to the adsorption geometry observed for THB annealed to 370 K, as becomes apparent in Fig. S1a (highlighted regions). The O 1s spectrum of DHBQ adsorbed on Cu(111) at RT bears very close resemblance to the one of the annealed THB, as demonstrated in Fig. S1b and thereby offers additional support for the conclusion that DHBQ is formed from THB as a result of annealing to 370 K. The binding energies of the two O 1s components are 532.5 eV and 530.7 eV (THB annealed to 370 K has virtually identical BEs of 532.6 eV and 530.8 eV). The C 1s spectrum in (c) exhibits two components with an intensity ratio of ~2:1 in favour for the high BE component at 285.3 eV over the low BE feature at 283.9 eV (THB: 285.4 eV and 284.0 eV). The C 1s spectrum of THB on Cu(111) before annealing is virtually identical to the one after annealing and hence is not provided separately.

### 3. Synchrotron-based XP Spectrum of THB on Cu(111) at RT

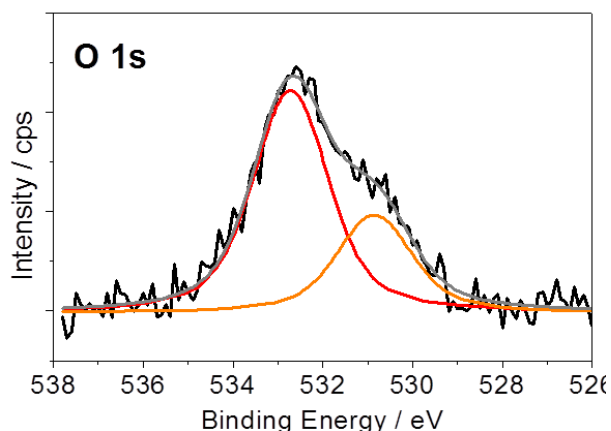


Fig. S2 Synchrotron XP (photon energy of 610 eV) spectrum of the O 1s region of THB adsorbed on Cu(111) after deposition of THB at RT.

The thermal load provided by the laboratory X-ray source caused a temperature increase of the sample as noted in the experimental section. Therefore, we provide the spectrum collected at a synchrotron facility (Astrid, located in Aarhus) that is void of this problem. The dehydrogenation level deduced from the spectrum (intensity ratio as judged from the areas under the peaks) amounts to 30%.

### 4. Computational Details

Density functional theory calculations were performed with the GPAW<sup>[2]</sup> software, a grid based implementation of the projector augmented wave method,<sup>[3]</sup> using the ASE interface.<sup>[4]</sup> To ensure convergence of relative energies a grid spacing of 0.16 Å was used. The meta-GGA functional M06-L<sup>[5]</sup> was used to describe the exchange and correlation contributions to the total energy, as it has previously been shown to give good results for the adsorption of aromatic molecules on transition metal surfaces.<sup>[6]</sup> 4 layers of copper with 25 atoms in each layer were used to model the surface. The bottom layer was fixed in the geometry of the bulk using the lattice constant of 3.59 Å obtained with the M06-L functional (to be compared with the experimental value of 3.61 Å<sup>[7]</sup>). Periodic boundary conditions were used in the x- and y-directions, while the z-direction remained aperiodic with a minimum of 6 Å of vacuum between the slab and the cell boundary. Starting configurations with the centre of the molecule at the top, bridge and hollow sites were tried for both the THB and the DHBQ molecule. Initial tests showed that the energy difference between adsorption configurations at fcc and hcp hollow sites were within the accuracy of the calculations and therefore only the fcc site was calculated at high accuracy. The molecule was oriented parallel to the surface and the 8 different orientations shown in Fig. S3a-h were tried for the bridge site, whereas only two different orientations were tried at the top(i-j) and the hollow(k-l) site due to the higher symmetry of these sites. In addition a vertical configuration(m-n) was tried for both molecules. This was found to have a considerably higher energy than the flat configuration with the lowest energy, and as the experimentally observed corrugation is not consistent with an upright orientation of the molecule, no exhaustive search in vertical configurations was performed.

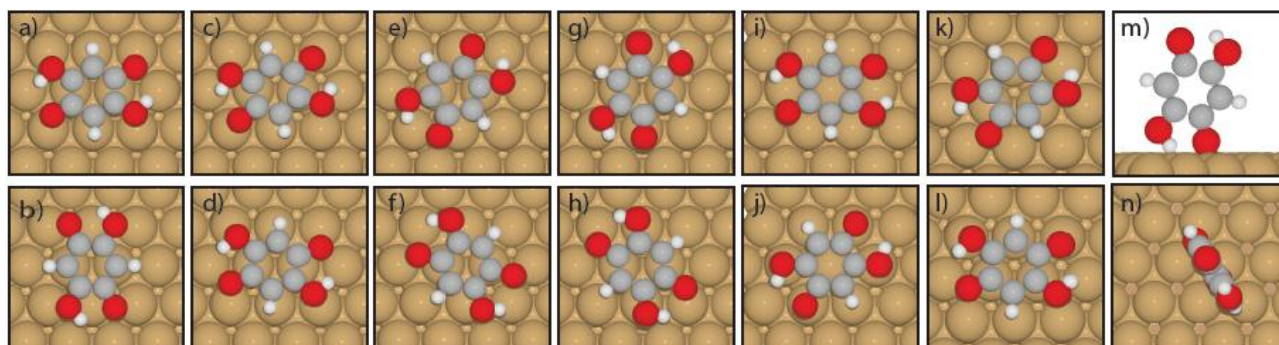


Figure S3: Calculated adsorption configurations for DHBQ at the bridge site a-h), top site i-j), hollow site k-l) as well as the calculated vertical configuration seen in side m) and top n) view.

All structures were relaxed down to a maximum force of 0.05 eV/Å with 2x2 k-points. The structure with the lowest energy was selected for both THB and DHBQ and relaxed with 4x4 k-points to get a more accurate value of the adsorption energy. This configuration was also used to make simulated STM images based on the Tersoff-Hamann model<sup>[8]</sup>, and for calculations of the core level shifts.

### Adsorption energies

The adsorption energies,  $E_{ads}$ , of the molecules are calculated as:

$$E_{ads} = E_{tot} - E_{Cu} - E_{THB} + n \cdot E_{H_2} \quad (1)$$

where  $E_{tot}$  is the total energy of the molecule on the surface and  $E_{Cu}$  and  $E_{THB}$  are the energies of the surface and the molecule respectively.  $E_{H_2}$  is the energy of a hydrogen molecule with  $n = 0$  for THB and  $n = 1$  for DHBQ.

The energy calculated by DFT concerns the electronic energy at 0 K only. To be able to compare the stability of THB and DHBQ, we need to consider the free energy of adsorption,  $F$ :

$$F = E_{ads} - T \cdot S \quad (2)$$

The entropies of THB and DHBQ are expected to be of a similar size and are therefore not included here, but the reaction also produces molecular hydrogen which has a high entropy in the gas phase, in particular at the low pressure in the STM chamber. The entropy of a hydrogen molecule at room temperature as a function of the pressure ( $p$ ) is given by:

$$S_{H_2}(p) = S_{H_2}^{\oplus} - R \cdot \ln\left(\frac{p}{p_0}\right) \quad (3)$$

where  $S_{H_2}^{\oplus}$  is the standard molar entropy of hydrogen<sup>[9]</sup> and  $p_0$  is the standard pressure. The exact pressure at the surface during the experiment is unknown, but a conservative estimate is  $10^{-9}$  mbar. The corresponding contribution to the free energy is -1.11 eV per  $H_2$  molecule at 298 K. The magnitude of the entropy term, and therefore also the pressure, is crucial to the energetic balance of the reaction. The maximum pressure at which the reaction would occur (neglecting zero point energy effects, see below) is found to be  $6 \cdot 10^{-7}$  mbar.

The reaction also changes the zero point energy (ZPE), but a full calculation of all vibrational modes is beyond the scope of this article. The dominating change is expected to be due to the high frequency stretching modes in  $H_2(g)$  ( $4400 \text{ cm}^{-1}$ <sup>[7]</sup>) and in the hydroxyl groups ( $\sim 3600 \text{ cm}^{-1}$ ). When the hydrogens from two hydroxyl groups of the THB molecule react to form a desorbing hydrogen molecule, these frequencies give rise to a change in zero point energy,  $\Delta ZPE$ :

$$\Delta ZPE(2 \cdot OH \rightarrow H_2) = \frac{1}{2} \cdot \hbar \cdot \omega_{H_2} - 2 \cdot \left(\frac{1}{2} \cdot \hbar \cdot \omega_{OH}\right) = -0.17 \text{ eV} \quad (4)$$

Some changes will also occur in the C-O and C-C vibrational modes, however the extent of these changes depends on how strongly the carbonyls bind to the surface. Some bond lengths found in the THB and DHBQ molecules on the surface and in the gas phase are given in table S1 (cf. Fig. S5 for numbering of the atoms). The relatively short Cu-O distance for the carbonyl oxygen (Cu(6)-O(9)) of DHBQ indicates a partial bond to the surface. This leads to an elongation of the carbonyl group (C(8)-O(9)) from 1.23 Å, typical of a double bond, when the molecule is in the gas phase, to 1.31 Å, which is intermediate between a single and a double bond, when the molecule is at the surface. This in turn influences the character of the bonding in the carbon ring, which is aromatic in the THB molecule when all C-O bonds are single bonds, but non-aromatic in DHBQ when two of the C-O bonds are double bonds. The interaction between DHBQ and the surface results in the C-C bond lengths becoming more similar, indicating that aromaticity is partially regained, however the remaining differences in C-C bond length and the buckling of the ring reveal that the pi-system is not fully restored.

The change in ZPE due to the changed character of the C-O and C-C bonds is therefore not easily estimated, but as the frequencies associated with these bonds are relatively small ( $< 2000 \text{ cm}^{-1}$ ), their contributions to  $\Delta ZPE$  are also expected to be small, and we consider the result in (4) a reasonable estimate of  $\Delta ZPE$ .

**Table S1:** Bond lengths in THB and DHBQ in Å. The numbering of the atoms is shown in figure S5.

	C(2)- O(5)	C(3)- O(4)	C(1)- C(2)	C(2)- C(3)	C(3)- C(1)	O(5)- Cu(6)	O(4)- Cu(7)	C(1)-Cu plane	C(2)-Cu plane	C(3)-Cu plane
THB (gas)	1.37	1.36	1.38	1.39	1.38	-	-	-	-	-
THB (surf)	1.37	1.36	1.39	1.39	1.39	3.23	3.03	2.86	2.88	2.86

	C(8)- O(9)	C(3)- O(10)	C(1)- C(8)	C(8)- C(3)	C(3)- C(1)	O(9)- Cu(6)	O(10)- Cu(7)	C(1)-Cu plane	C(8)-Cu plane	C(3)-Cu plane
DHBQ(gas)	1.23	1.32	1.43	1.50	1.35	-	-	-	-	-
DHBQ(surf)	1.31	1.35	1.42	1.43	1.39	2.27	2.79	2.30	2.21	2.34

#### Core level shifts

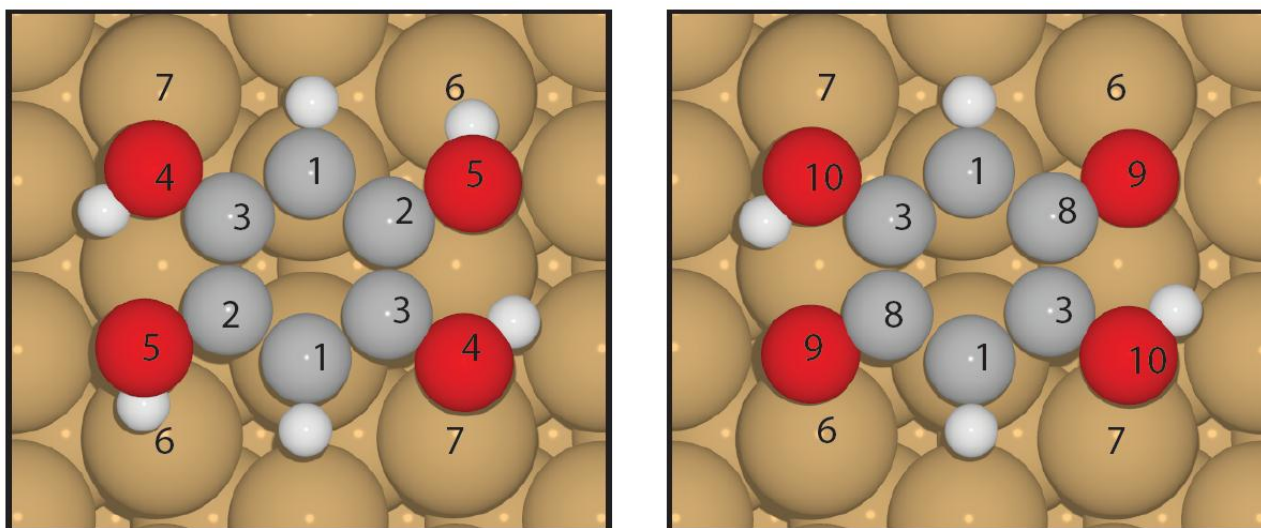


**Figure S4:** Numbering of atoms in THB(left) and DHBQ (right).

Core level shifts were calculated as the difference in total energy when one electron is removed from the 1s level of a selected atom ( $E_{atom}$ ), compared to the energy when the core electron is removed on a reference atom ( $E_{ref}$ ). The carbon bound to hydrogen (C(1) in Fig. S4) and the oxygen in the alcohol group (O(4) in Fig. S4) are used as reference atoms for the C1s and O1s shifts respectively. The sign convention is that a positive shift represents a shift towards higher binding energies, giving that:

$$\Delta_{CL} = E_{atom} - E_{ref} \quad (5)$$

The core level shifts calculated for the single (isolated) molecule on the surface in the optimised adsorption geometry are given in table S2. The core level shift calculations for an isolated DHBQ molecule on the surface predict a BE that is 2.95 eV higher for the hydroxyl oxygen compared to the carbonyl oxygen. This confirms the assignment of the experimental peaks, though the magnitude of the shift is overestimated. As the intermolecular hydrogen bonding affects the adsorption geometry and electronic structure, only a qualitative agreement with experiment is expected. In fact, a reduction in the difference of the core level binding energies of up to 1 eV for different oxygen species (C=O and C-O-H) in formic acid due to hydrogen bonding interactions have been reported in literature.<sup>[10]</sup> Similarly, hydrogen bonding between hydroxyl and carbonyl groups in the DHBQ overlayer is thought to reduce the difference in O1s binding energy between these two species in an analogous fashion. Taking this into account, the calculations agree reasonably well with the experimental value. The C1s shifts show almost perfect agreement with experiment, predicting peak separations of 1.26 eV between C3 and C1 carbons (cf. Fig. 4b for labelling) and 1.34 eV between C2 and C1 carbons. This renders the experimental observation of a single peak, comprising both C2 and C3 species, plausible.

**Table S2:** Calculated values of the core level shifts in eV as well as the experimental values at RT. The numbering of the atoms is shown in figure S4.

	C(2)	C(3)	O(5)
Exp	1.4	1.4	1.9 (THB) /1.8 (DHBQ)
Calc. THB	1.50	1.50	-
Calc (DHBQ)	1.26	1.34	2.95

### Structural model

The structural model is based on the optimised hydrogen bonding pattern in the gas phase. To calculate this, one molecule is placed in a unit cell with  $|a| = |b| = 7.5 \text{ \AA}$  and  $\angle(a, b) = 60^\circ$ , corresponding to the experimentally observed unit cell, and periodic boundary conditions. The molecule is rotated in steps of  $4^\circ$ , thereby probing all possible structures under the assumption that all molecules have the same orientation. The orientation is kept fixed by fixing the two carbon atoms on either side of the ring that are bound to hydrogen (C1 in Fig. S4), and the rest of the molecule is relaxed freely. The energy as a function of the orientation shows a clear minimum when the molecules form parallel rows inter-linked via double hydrogen bonds. As the experiment does not exclude a structure where the molecules have different orientations, all possible combinations of orientations (in steps of  $10^\circ$ ) for two molecules in a unit cell were also tried. However, the lowest energy was still found when both molecules have the same orientation. The optimised gas phase structure is transferred to a  $22.5 \times 22.5 \text{ \AA}^2$  slab of copper with an orientation with respect to the Cu<110> direction of  $17^\circ$  (Fig. S5). This slab is the smallest possible able to accommodate an integer multiple of the experimentally observed unit cells for the overlayer. Since the molecular overlayer and the substrate are not directly commensurate, the molecules occupy inequivalent adsorption sites within the computational unit cell. Due to the large size of the cell the structure is only relaxed on two layers of copper with 2x2 k-points meaning that the calculated total energy gain from adsorption and hydrogen bonding is not sufficiently accurate to be included in this discussion.

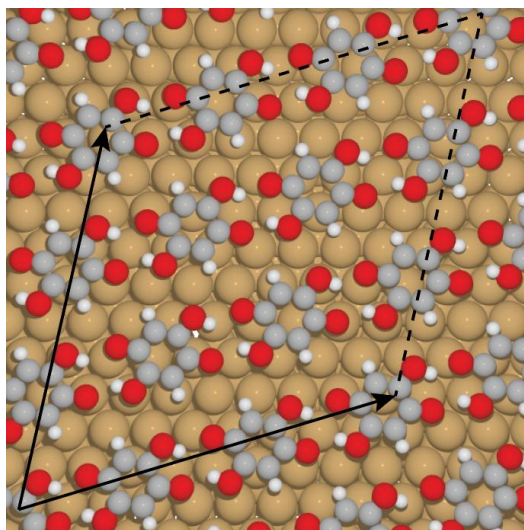


**Figure S5:** DHBQ overlayer structure. The computational unit cell is marked.

### Adsorption structures for 4,5-dihydroxybenzo-1,2-dione

The molecule 4,5-dihydroxybenzo-1,2-dione has the same stoichiometry as DHBQ (2,5-dihydroxybenzo-1,4-dione) and is expected to provide a very similar XPS signal. It might therefore be considered an alternative dehydrogenation product. However, oxidation of hydroxybenzenes generally leads to para-quinone derivatives while ortho-quinones are synthesized by more complicated multi-step approaches. The reason is stabilization of the p-semiquinone intermediate in contrast to the o-semiquinone owing to charge separation. From organic synthesis considerations DHBQ is thus the anticipated dehydrogenation product. We nevertheless performed calculations for adsorbed 4,5-dihydroxybenzo-1,2-dione as reported in Fig. S6. For an isolated molecule, an upright configuration is most stable (Fig. S6a-b) with a binding energy of  $-1.51 \text{ eV}$  (comp.  $-1.31 \text{ eV}$  for DHBQ), but an upright geometry does not allow for hydrogen bonding. The second best geometry (Fig. S6c-d) with a binding energy of  $-1.38 \text{ eV}$  has a tilt of  $\sim 21^\circ$  which leads to a slight asymmetry in the simulated STM-images (Fig. S6e). Hydrogen-bonded structures were made for DHBQ and for 4,5-dihydroxybenzo-1,2-dione in a commensurate  $3 \times 3$  cell (approximating the experimentally observed unit cell size), in both cases such that each molecule makes two hydrogen bonds to one of its neighbours (Fig. S4f-g). In these calculations the DHBQ structure is more stable by  $0.23 \text{ eV}$ . From the higher stability of the hydrogen-bonded phase for DHBQ and the good agreement in the STM data for DHBQ and annealed THB we conclude the dehydrogenation product is DHBQ.

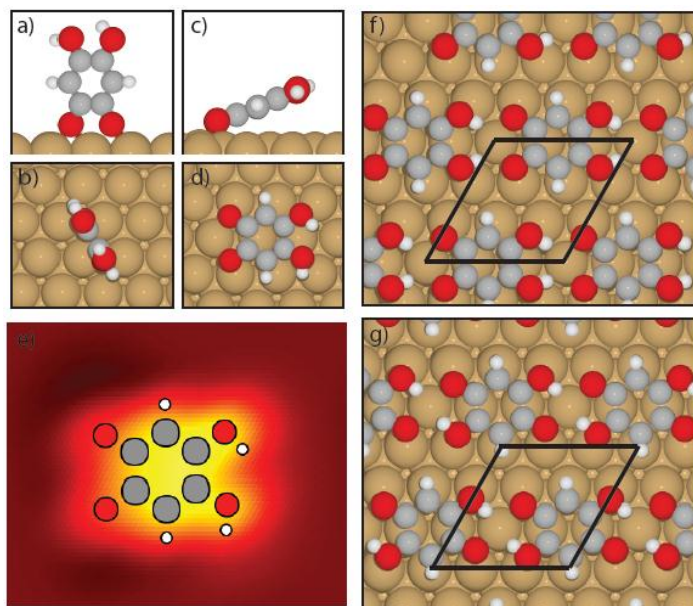


**Figure S6:** Most stable adsorption configuration for 4,5-dihydroxybenzo-1,2-dione in side (a) and top (b) view. The most stable non-vertical adsorption geometry (c-d) gives rise to an asymmetry in the simulated STM image (e). Hydrogen bonded structures of 4,5-dihydroxybenzo-1,2-dione (f) and DHBQ (g) are calculated in the commensurate unit cell marked in black.

#### Coordinates

Coordinates of optimised structures:

#### THB on Cu, 4x4:

E = -952.3449

0 Cu	0.0000	0.0000	7.0000
1 Cu	2.5385	0.0000	7.0000
2 Cu	5.0770	0.0000	7.0000
3 Cu	7.6155	0.0000	7.0000
4 Cu	10.1541	0.0000	7.0000
5 Cu	1.2693	2.1984	7.0000
6 Cu	3.8078	2.1984	7.0000
7 Cu	6.3463	2.1984	7.0000
8 Cu	8.8848	2.1984	7.0000
9 Cu	11.4233	2.1984	7.0000
10 Cu	2.5385	4.3968	7.0000
11 Cu	5.0770	4.3968	7.0000
12 Cu	7.6155	4.3968	7.0000
13 Cu	10.1541	4.3968	7.0000
14 Cu	12.6926	4.3968	7.0000
15 Cu	3.8078	6.5953	7.0000
16 Cu	6.3463	6.5953	7.0000
17 Cu	8.8848	6.5953	7.0000
18 Cu	11.4233	6.5953	7.0000
19 Cu	13.9618	6.5953	7.0000
20 Cu	5.0770	8.7937	7.0000
21 Cu	7.6155	8.7937	7.0000
22 Cu	10.1541	8.7937	7.0000
23 Cu	12.6926	8.7937	7.0000
24 Cu	15.2311	8.7937	7.0000
25 Cu	1.2811	0.7371	9.0509
26 Cu	3.8140	0.7235	9.0520
27 Cu	6.3440	0.7371	9.0532
28 Cu	8.8761	0.7221	9.0516
29 Cu	11.4150	0.7359	9.0518

30 Cu	2.5323	2.9405	9.0508
31 Cu	5.0696	2.9262	9.0587
32 Cu	7.6234	2.9273	9.0591
33 Cu	10.1574	2.9420	9.0517
34 Cu	12.6914	2.9259	9.0598
35 Cu	3.8091	5.1255	9.0502
36 Cu	6.3450	5.1343	9.0542
37 Cu	8.8803	5.1265	9.0528
38 Cu	11.4224	5.1339	9.0557
39 Cu	13.9525	5.1289	9.0577
40 Cu	5.0642	7.3270	9.0509
41 Cu	7.6262	7.3268	9.0494
42 Cu	10.1560	7.3235	9.0570
43 Cu	12.6918	7.3276	9.0604
44 Cu	15.2271	7.3271	9.0562
45 Cu	6.3460	9.5188	9.0541
46 Cu	8.8800	9.5287	9.0589
47 Cu	11.4174	9.5180	9.0551
48 Cu	13.9593	9.5229	9.0570
49 Cu	16.5040	9.5284	9.0628
50 Cu	0.0099	1.4616	11.0986
51 Cu	2.5349	1.4627	11.1085
52 Cu	5.0740	1.4680	11.1145
53 Cu	7.6038	1.4635	11.1058
54 Cu	10.1630	1.4612	11.0962
55 Cu	1.2809	3.6615	11.1138
56 Cu	3.8044	3.6606	11.1086
57 Cu	6.3444	3.6624	11.1212
58 Cu	8.8829	3.6757	11.1135
59 Cu	11.4174	3.6657	11.1059
60 Cu	2.5333	5.8646	11.1159
61 Cu	5.0662	5.8541	11.0981
62 Cu	7.6118	5.8606	11.1004
63 Cu	10.1648	5.8686	11.1226
64 Cu	12.6947	5.8556	11.1184
65 Cu	3.8146	8.0525	11.1171
66 Cu	6.3465	8.0701	11.0993
67 Cu	8.8801	8.0606	11.1062
68 Cu	11.4172	8.0672	11.1149
69 Cu	13.9736	8.0673	11.1165
70 Cu	5.0728	10.2549	11.1140
71 Cu	7.6248	10.2562	11.1122
72 Cu	10.1600	10.2719	11.1112
73 Cu	12.6908	10.2529	11.1127
74 Cu	15.2293	10.2681	11.1159
75 Cu	0.0021	0.0011	13.1678
76 Cu	2.5325	0.0012	13.1681
77 Cu	5.0623	-0.0012	13.1676
78 Cu	7.6311	-0.0038	13.1607
79 Cu	10.1646	0.0005	13.1705
80 Cu	1.2761	2.1905	13.1695
81 Cu	3.8142	2.2026	13.1693
82 Cu	6.3413	2.1784	13.1771
83 Cu	8.8893	2.1908	13.1211
84 Cu	11.4623	2.1997	13.1299
85 Cu	2.5324	4.3849	13.1688
86 Cu	5.0567	4.4059	13.1631
87 Cu	7.6004	4.3975	13.1605
88 Cu	10.1707	4.3865	13.1587
89 Cu	12.7010	4.4042	13.1648
90 Cu	3.8160	6.6073	13.1704
91 Cu	6.3316	6.5931	13.1273
92 Cu	8.8747	6.6166	13.1334
93 Cu	11.4557	6.6161	13.1772

94 Cu	13.9782	6.5919	13.1714
95 Cu	5.0821	8.7988	13.1719
96 Cu	7.6110	8.8004	13.1688
97 Cu	10.1568	8.7978	13.1570
98 Cu	12.6972	8.8112	13.1693
99 Cu	15.2274	8.7917	13.1745
100 O	7.6610	6.8722	16.1100
101 O	10.3405	6.7364	15.9818
102 O	7.4325	2.0734	16.0203
103 O	10.1162	1.9456	16.1054
104 C	10.2763	4.3702	16.0160
105 C	7.4949	4.4416	16.0322
106 C	9.5515	3.1886	16.0422
107 C	8.1585	3.2216	16.0300
108 C	9.6127	5.5896	16.0122
109 C	8.2201	5.6243	16.0426
110 H	11.3413	4.3563	16.0236
111 H	6.4303	4.4536	16.0511
112 H	6.8041	6.8807	15.6575
113 H	9.7218	7.4752	15.8698
114 H	8.0467	1.3335	15.8913
115 H	10.9893	1.9574	15.6864

**DHBQ on Cu, 4x4:**

E = -944.2071

0 Cu	0.0000	0.0000	7.0000
1 Cu	2.5385	0.0000	7.0000
2 Cu	5.0770	0.0000	7.0000
3 Cu	7.6155	0.0000	7.0000
4 Cu	10.1541	0.0000	7.0000
5 Cu	1.2693	2.1984	7.0000
6 Cu	3.8078	2.1984	7.0000
7 Cu	6.3463	2.1984	7.0000
8 Cu	8.8848	2.1984	7.0000
9 Cu	11.4233	2.1984	7.0000
10 Cu	2.5385	4.3968	7.0000
11 Cu	5.0770	4.3968	7.0000
12 Cu	7.6155	4.3968	7.0000
13 Cu	10.1541	4.3968	7.0000
14 Cu	12.6926	4.3968	7.0000
15 Cu	3.8078	6.5953	7.0000
16 Cu	6.3463	6.5953	7.0000
17 Cu	8.8848	6.5953	7.0000
18 Cu	11.4233	6.5953	7.0000
19 Cu	13.9618	6.5953	7.0000
20 Cu	5.0770	8.7937	7.0000
21 Cu	7.6155	8.7937	7.0000
22 Cu	10.1541	8.7937	7.0000
23 Cu	12.6926	8.7937	7.0000
24 Cu	15.2311	8.7937	7.0000
25 Cu	1.2678	0.7434	9.0481
26 Cu	3.8071	0.7319	9.0327
27 Cu	6.3414	0.7422	9.0399
28 Cu	8.8779	0.7291	9.0415
29 Cu	11.4169	0.7415	9.0465
30 Cu	2.5337	2.9458	9.0392
31 Cu	5.0691	2.9314	9.0373
32 Cu	7.6208	2.9323	9.0368
33 Cu	10.1585	2.9454	9.0456
34 Cu	12.6911	2.9302	9.0550
35 Cu	3.8192	5.1353	9.0528
36 Cu	6.3440	5.1437	9.0483
37 Cu	8.8764	5.1291	9.0422



38 Cu	11.4296	5.1275	9.0492
39 Cu	13.9708	5.1433	9.0444
40 Cu	5.0649	7.3296	9.0541
41 Cu	7.6229	7.3265	9.0455
42 Cu	10.1531	7.3243	9.0357
43 Cu	12.6902	7.3288	9.0449
44 Cu	15.2255	7.3460	9.0418
45 Cu	6.3440	9.5105	9.0479
46 Cu	8.8758	9.5333	9.0311
47 Cu	11.4097	9.5193	9.0343
48 Cu	13.9456	9.5326	9.0410
49 Cu	16.5011	9.5340	9.0479
50 Cu	-0.0049	1.4944	11.1279
51 Cu	2.5309	1.4757	11.0820
52 Cu	5.0590	1.4827	11.0815
53 Cu	7.5960	1.4667	11.0800
54 Cu	10.1711	1.4638	11.0902
55 Cu	1.2874	3.6737	11.0894
56 Cu	3.8132	3.6909	11.0870
57 Cu	6.3423	3.6644	11.0889
58 Cu	8.8768	3.6882	11.0954
59 Cu	11.4089	3.6587	11.1240
60 Cu	2.5374	5.8753	11.0949
61 Cu	5.1079	5.8831	11.1367
62 Cu	7.5944	5.8716	11.1080
63 Cu	10.1608	5.8772	11.0881
64 Cu	12.6936	5.8636	11.0925
65 Cu	3.8089	8.0634	11.0961
66 Cu	6.3501	8.0702	11.1212
67 Cu	8.8770	8.0920	11.0715
68 Cu	11.4081	8.0752	11.0821
69 Cu	13.9675	8.0719	11.0913
70 Cu	5.0786	10.2683	11.0916
71 Cu	7.6104	10.2758	11.0840
72 Cu	10.1526	10.2869	11.0723
73 Cu	12.6789	10.2580	11.0775
74 Cu	15.2242	10.2760	11.0921
75 Cu	0.0070	0.0035	13.1457
76 Cu	2.5290	0.0437	13.1360
77 Cu	5.0542	0.0066	13.1351
78 Cu	7.5910	-0.0321	13.1164
79 Cu	10.1476	-0.0311	13.1525
80 Cu	1.2935	2.2359	13.1517
81 Cu	3.8150	2.2138	13.1361
82 Cu	6.3205	2.1634	13.1239
83 Cu	8.8899	2.1554	13.0508
84 Cu	11.4617	2.1929	13.2474
85 Cu	2.5403	4.4086	13.1493
86 Cu	5.0443	4.4118	13.1361
87 Cu	7.5732	4.3705	13.1098
88 Cu	10.1700	4.4592	13.1114
89 Cu	12.7128	4.4172	13.1299
90 Cu	3.8103	6.6185	13.1527
91 Cu	6.3307	6.6559	13.2665
92 Cu	8.8784	6.6563	13.0567
93 Cu	11.4716	6.6421	13.1315
94 Cu	13.9787	6.5990	13.1463
95 Cu	5.0549	8.8265	13.1460
96 Cu	7.6388	8.8483	13.1478
97 Cu	10.1634	8.8534	13.1109
98 Cu	12.6928	8.8202	13.1361
99 Cu	15.2177	8.7884	13.1431
100 O	7.5281	1.9984	15.6314
101 O	10.1919	1.9812	15.1327

102 O	7.5506	6.7661	15.1563
103 O	10.2185	6.7444	15.6246
104 C	10.2782	4.3766	15.4346
105 C	7.4646	4.3679	15.4482
106 C	9.5605	5.5702	15.4829
107 C	8.1391	5.6087	15.3478
108 C	9.6021	3.1358	15.3399
109 C	8.1834	3.1735	15.4899
110 H	11.3353	4.3855	15.5646
111 H	6.4074	4.3574	15.5749
112 H	8.2053	1.2974	15.5668
113 H	9.5407	7.4455	15.5731

**DHB+2H(ads):**

E = -951.7786

0 Cu	0.0000	0.0000	7.0000
1 Cu	2.5385	0.0000	7.0000
2 Cu	5.0770	0.0000	7.0000
3 Cu	7.6155	0.0000	7.0000
4 Cu	10.1541	0.0000	7.0000
5 Cu	1.2693	2.1984	7.0000
6 Cu	3.8078	2.1984	7.0000
7 Cu	6.3463	2.1984	7.0000
8 Cu	8.8848	2.1984	7.0000
9 Cu	11.4233	2.1984	7.0000
10 Cu	2.5385	4.3968	7.0000
11 Cu	5.0770	4.3968	7.0000
12 Cu	7.6155	4.3968	7.0000
13 Cu	10.1541	4.3968	7.0000
14 Cu	12.6926	4.3968	7.0000
15 Cu	3.8078	6.5953	7.0000
16 Cu	6.3463	6.5953	7.0000
17 Cu	8.8848	6.5953	7.0000
18 Cu	11.4233	6.5953	7.0000
19 Cu	13.9618	6.5953	7.0000
20 Cu	5.0770	8.7937	7.0000
21 Cu	7.6155	8.7937	7.0000
22 Cu	10.1541	8.7937	7.0000
23 Cu	12.6926	8.7937	7.0000
24 Cu	15.2311	8.7937	7.0000
25 Cu	1.2706	0.7404	9.0409
26 Cu	3.8115	0.7235	9.0352
27 Cu	6.3423	0.7410	9.0443
28 Cu	8.8763	0.7234	9.0505
29 Cu	11.4122	0.7409	9.0415
30 Cu	2.5321	2.9473	9.0406
31 Cu	5.0673	2.9295	9.0444
32 Cu	7.6193	2.9319	9.0417
33 Cu	10.1578	2.9442	9.0466
34 Cu	12.6894	2.9300	9.0502
35 Cu	3.8171	5.1341	9.0513
36 Cu	6.3388	5.1463	9.0601
37 Cu	8.8746	5.1246	9.0522
38 Cu	11.4311	5.1279	9.0638
39 Cu	13.9526	5.1294	9.0515
40 Cu	5.0664	7.3276	9.0521
41 Cu	7.6242	7.3242	9.0488
42 Cu	10.1556	7.3077	9.0428
43 Cu	12.6906	7.3287	9.0441
44 Cu	15.2266	7.3413	9.0394
45 Cu	6.3433	9.5076	9.0447
46 Cu	8.8794	9.5264	9.0312
47 Cu	11.4059	9.5134	9.0443

48 Cu	13.9512	9.5336	9.0385
49 Cu	16.5066	9.5375	9.0556
50 Cu	-0.0060	1.4949	11.1051
51 Cu	2.5309	1.4726	11.0738
52 Cu	5.0585	1.4758	11.0856
53 Cu	7.5931	1.4628	11.0856
54 Cu	10.1682	1.4604	11.0889
55 Cu	1.2813	3.6633	11.1111
56 Cu	3.8094	3.6919	11.0874
57 Cu	6.3405	3.6653	11.0932
58 Cu	8.8805	3.6644	11.1127
59 Cu	11.4072	3.6595	11.1239
60 Cu	2.5315	5.8749	11.0860
61 Cu	5.0689	5.9047	11.1591
62 Cu	7.5858	5.8651	11.1176
63 Cu	10.1571	5.8689	11.1039
64 Cu	12.7036	5.8929	11.1186
65 Cu	3.8065	8.0787	11.0884
66 Cu	6.3499	8.0679	11.1169
67 Cu	8.8782	8.0732	11.0760
68 Cu	11.4092	8.0710	11.0845
69 Cu	13.9741	8.0757	11.0845
70 Cu	5.1106	10.2838	11.1099
71 Cu	7.6186	10.2685	11.0722
72 Cu	10.1383	10.2830	11.1001
73 Cu	12.6801	10.2522	11.0757
74 Cu	15.2294	10.2619	11.1132
75 Cu	0.0147	0.0038	13.1699
76 Cu	2.5251	0.0370	13.1740
77 Cu	5.0503	0.0003	13.1346
78 Cu	7.5825	-0.0415	13.1136
79 Cu	10.1539	-0.0457	13.1413
80 Cu	1.2687	2.1928	13.1753
81 Cu	3.8209	2.2138	13.1239
82 Cu	6.3164	2.1596	13.1309
83 Cu	8.8742	2.1244	13.0665
84 Cu	11.4137	2.1783	13.2160
85 Cu	2.5292	4.3745	13.1394
86 Cu	5.0431	4.4111	13.1348
87 Cu	7.5706	4.3609	13.1188
88 Cu	10.1637	4.4525	13.1230
89 Cu	12.7092	4.4124	13.1235
90 Cu	3.7939	6.6197	13.1875
91 Cu	6.3260	6.6482	13.2600
92 Cu	8.8722	6.6469	13.0666
93 Cu	11.4721	6.6372	13.1394
94 Cu	13.9872	6.5959	13.1853
95 Cu	5.0784	8.8260	13.1241
96 Cu	7.6423	8.8330	13.1322
97 Cu	10.1616	8.8220	13.1138
98 Cu	12.6815	8.8180	13.1253
99 Cu	15.2172	8.7790	13.1887
100 O	7.5282	1.9992	15.6378
101 O	10.1871	1.9807	15.1333
102 O	7.5525	6.7651	15.1608
103 O	10.2191	6.7440	15.6326
104 C	10.2814	4.3777	15.4385
105 C	7.4619	4.3664	15.4430
106 C	9.5606	5.5698	15.4916
107 C	8.1387	5.6079	15.3555
108 C	9.6033	3.1369	15.3470
109 C	8.1834	3.1742	15.4899
110 H	11.3389	4.3862	15.5698
111 H	6.4051	4.3577	15.5806

112 H	8.2032	1.2970	15.5692
113 H	9.5427	7.4457	15.5746
114 H	15.2215	7.3342	14.1695
115 H	1.2561	0.7371	14.1544

**Cu slab, 4x4:**

E = -829.9448

0 Cu	0.0000	0.0000	7.0000
1 Cu	2.5385	0.0000	7.0000
2 Cu	5.0770	0.0000	7.0000
3 Cu	7.6155	0.0000	7.0000
4 Cu	10.1541	0.0000	7.0000
5 Cu	1.2693	2.1984	7.0000
6 Cu	3.8078	2.1984	7.0000
7 Cu	6.3463	2.1984	7.0000
8 Cu	8.8848	2.1984	7.0000
9 Cu	11.4233	2.1984	7.0000
10 Cu	2.5385	4.3968	7.0000
11 Cu	5.0770	4.3968	7.0000
12 Cu	7.6155	4.3968	7.0000
13 Cu	10.1541	4.3968	7.0000
14 Cu	12.6926	4.3968	7.0000
15 Cu	3.8078	6.5953	7.0000
16 Cu	6.3463	6.5953	7.0000
17 Cu	8.8848	6.5953	7.0000
18 Cu	11.4233	6.5953	7.0000
19 Cu	13.9618	6.5953	7.0000
20 Cu	5.0770	8.7937	7.0000
21 Cu	7.6155	8.7937	7.0000
22 Cu	10.1541	8.7937	7.0000
23 Cu	12.6926	8.7937	7.0000
24 Cu	15.2311	8.7937	7.0000
25 Cu	1.2756	0.7365	9.0676
26 Cu	3.8116	0.7240	9.0656
27 Cu	6.3457	0.7373	9.0686
28 Cu	8.8787	0.7237	9.0655
29 Cu	11.4148	0.7366	9.0673
30 Cu	2.5328	2.9390	9.0656
31 Cu	5.0670	2.9255	9.0674
32 Cu	7.6232	2.9260	9.0672
33 Cu	10.1582	2.9391	9.0657
34 Cu	12.6916	2.9267	9.0720
35 Cu	3.8114	5.1268	9.0686
36 Cu	6.3456	5.1389	9.0672
37 Cu	8.8794	5.1265	9.0683
38 Cu	11.4237	5.1312	9.0673
39 Cu	13.9572	5.1300	9.0670
40 Cu	5.0661	7.3274	9.0655
41 Cu	7.6244	7.3277	9.0657
42 Cu	10.1556	7.3276	9.0673
43 Cu	12.6917	7.3276	9.0729
44 Cu	-0.00009	-0.00654	-0.03061
45 Cu	0.00175	0.02717	-0.02204
46 Cu	0.04067	-0.02160	-0.03335
47 Cu	-0.00067	-0.00112	-0.03094
48 Cu	-0.00571	0.00320	-0.03060
49 Cu	-0.03929	-0.02269	-0.03347
50 Cu	-0.00120	-0.03842	-0.04870
51 Cu	0.02583	0.01491	-0.06127
52 Cu	0.00605	-0.00718	-0.04539
53 Cu	0.00218	-0.00036	-0.04544
54 Cu	-0.02688	0.01444	-0.06169

55 Cu	-0.05097	-0.00737	-0.03735
56 Cu	-0.00319	0.00882	-0.04539
57 Cu	-0.00173	-0.00100	-0.03468
58 Cu	0.00408	0.00841	-0.04572
59 Cu	0.04813	-0.00542	-0.03726
60 Cu	0.03549	-0.02130	-0.03401
61 Cu	0.00078	0.00207	-0.04544
62 Cu	0.00933	-0.00067	-0.04572
63 Cu	-0.03674	-0.02121	-0.03382
64 Cu	-0.00185	0.03272	-0.04710
65 Cu	-0.02112	0.04420	-0.03863
66 Cu	-0.00094	-0.03049	-0.06169
67 Cu	0.01937	0.04440	-0.03726
68 Cu	0.02741	-0.01796	-0.04710
69 Cu	-0.02922	-0.01687	-0.04754
70 Cu	0.03102	0.01791	-0.05022
71 Cu	-0.03387	0.01818	-0.04870
72 Cu	-0.03187	-0.04045	-0.03735
73 Cu	-0.00071	0.04139	-0.03401
74 Cu	0.02772	-0.04039	-0.03863
75 Cu	0.00085	0.00049	-0.00876
76 Cu	0.00682	0.00281	-0.00476
77 Cu	0.04824	0.00052	-0.01512
78 Cu	-0.04749	0.00117	-0.01623
79 Cu	-0.00486	0.00369	-0.00596
80 Cu	0.00584	0.00450	-0.00476
81 Cu	-0.04219	-0.02436	-0.00414
82 Cu	0.00109	0.02818	-0.00973
83 Cu	0.04238	-0.02364	-0.00344
84 Cu	-0.00239	0.00380	-0.00437
85 Cu	0.02457	0.04151	-0.01512
86 Cu	0.02494	-0.01315	-0.00973
87 Cu	-0.02305	-0.01331	-0.00893
88 Cu	-0.02432	0.04290	-0.01543
89 Cu	0.00042	-0.04814	-0.00728
90 Cu	-0.02273	-0.04171	-0.01623
91 Cu	0.00072	0.04852	-0.00344
92 Cu	0.02499	-0.04251	-0.01543
93 Cu	0.02620	0.01513	-0.01365
94 Cu	-0.02381	0.01384	-0.01462
95 Cu	0.00076	-0.00605	-0.00596
96 Cu	0.00209	-0.00397	-0.00437
97 Cu	-0.04148	0.02443	-0.00728
98 Cu	0.00009	-0.02754	-0.01462
99 Cu	0.04338	0.02505	-0.00596

**THB gas phase:**

E = -121.4169

0 O	21.4641	12.3017	11.9510
1 O	21.4094	9.5852	11.9510
2 O	16.6781	12.4029	11.9510
3 O	16.6235	9.6871	11.9510
4 C	19.0455	9.6102	11.9510
5 C	19.0423	12.3783	11.9510
6 C	17.8517	10.3034	11.9510
7 C	17.8418	11.6915	11.9510
8 C	20.2458	10.2974	11.9510
9 C	20.2360	11.6852	11.9510
10 H	19.0583	8.5452	11.9510
11 H	19.0293	13.4433	11.9510
12 H	21.3269	13.2522	11.9510
13 H	22.1388	10.2139	11.9510
14 H	15.9503	11.7721	11.9510

15 H 16.7599 8.7363 11.9510

**DHB gas phase:**

E = -113.4823

0 O 21.3952 12.3327 11.9510  
1 O 21.3795 9.7473 11.9510  
2 O 16.6983 12.2371 11.9510  
3 O 16.6826 9.6515 11.9510  
4 C 19.0268 9.5343 11.9510  
5 C 19.0510 12.4500 11.9510  
6 C 17.8709 10.2270 11.9510  
7 C 17.8198 11.7295 11.9510  
8 C 20.2580 10.2548 11.9510  
9 C 20.2070 11.7573 11.9510  
10 H 19.0504 8.4717 11.9510  
11 H 19.0273 13.5125 11.9510  
12 H 22.0330 11.5903 11.9510  
13 H 16.0447 10.3939 11.9510

**H<sub>2</sub> gas phase:**

E = -7.1843

0 H 18.6780 11.0054 11.9510  
1 H 19.3997 10.9787 11.9510

**Notes and references**

- [1] P. R. Weider, L. S. Hegedus, H. Asada, S. V. Dandreq, *J Org Chem* 1985, **50**, 4276-4281.
- [2] aJ. Enkovaara, C. Rostgaard, J. J. Mortensen, J. Chen, M. Dulak, L. Ferrighi, J. Gavnholt, C. Glinsvad, V. Haikola, H. A. Hansen, H. H. Kristoffersen, M. Kuisma, A. H. Larsen, L. Lehtovaara, M. Ljungberg, O. Lopez-Acevedo, P. G. Moses, J. Ojanen, T. Olsen, V. Petzold, N. A. Romero, J. Stausholm-Moller, M. Strange, G. A. Tritsarlis, M. Vanin, M. Walter, B. Hammer, H. Hakkinen, G. K. H. Madsen, R. M. Nieminen, J. Norskov, M. Puska, T. T. Rantala, J. Schiotz, K. S. Thygesen, K. W. Jacobsen, *J Phys-Condens Mat* 2010, **22**; bJ. J. Mortensen, L. B. Hansen, K. W. Jacobsen, *Phys Rev B* 2005, **71**.
- [3] P. E. Blöchl, *Phys Rev B* 1994, **50**, 17953-17979.
- [4] S. R. Bahn, K. W. Jacobsen, *Comput Sci Eng* 2002, **4**, 56-66.
- [5] Y. Zhao, D. G. Truhlar, *J Chem Phys* 2006, **125**.
- [6] L. Ferrighi, G. K. H. Madsen, B. Hammer, *J Chem Phys* 2011, **135**.
- [7] American Institute of Physics., D. E. Gray, *American Institute of Physics handbook. Section editors: Bruce H. Billings [and others] Coordinating editor: Dwight E. Gray*, 3d ed., McGraw-Hill, New York,, 1972.
- [8] J. Tersoff, D. R. Hamann, *Phys Rev B* 1985, **31**, 805-813.
- [9] D. D. Wagman, W. H. Evans, V. B. Parker, R. H. Schumm, I. Halow, S. M. Bailey, K. L. Churney, R. L. Nuttall, *J Phys Chem Ref Data* 1982, **11**, 1-&.
- [10] aP. Aplincourt, C. Bureau, J. L. Anthoine, D. P. Chong, *J Phys Chem A* 2001, **105**, 7364-7370; bS. Garcia-Gil, A. Arnau, A. Garcia-Lekue, *Surf Sci* 2013, **613**, 102-107.